

Simulating the Electrophysiology of Rabbit Atrial Cells

Modelling the Pathways of Interatrial Conduction and Investigating the Causes of Spontaneous Action Potentials

Deborah A. Cheverton and Robert D. Robinson

Supervised by H. Zhang

School of Physics and Astronomy

The University of Manchester

Manchester M13 9PL

Submitted as partial contribution to MPhys (Hons) Physics

January 2009

ABSTRACT

Heart disease is the single most common cause of death in western society so understanding heart function is vitally important. A complete model of cardiac electrophysiology would provide pharmacologists with a powerful tool for drug development and testing .In Section A, data from physiological studies of rabbit cardiomyocytes from the major interatrial conduction pathways, Bachmann's bundle and the coronary sinus, and the pulmonary vein was used to create mathematical models of the electrophysiology of these cell types. Ionic currents studied included I_{Kr} , I_{Ks} , I_{to} , I_{CaL} , I_{CaT} . After fitting to available experimental data the formulae for individual single currents were compiled into a complete single cell code which allowed us to successfully recreate single-cell action potentials of Bachmann's bundle and pulmonary vein cells as well as a reasonable approximation to the single action potential of cells in the coronary sinus. In Section B we consider the unique electrophysiological characteristics of pulmonary vein cells that have been shown to experience spontaneous electrical activity. The pulmonary vein model constructed in Section A was extended to include new currents I_f and I_{ClCa} . I_{NaCa} was altered to better fit experimental data. We conclude that changes in intracellular calcium dynamics and the resulting calcium activated depolarising current, I_{ti} , are the primary cause of spontaneous activity and suggest lines of inquiry to provide further support for this theory.

KEY WORDS: Ion Channel • Action Potential • Bachmann's Bundle • Coronary Sinus • Pulmonary Vein • Atrial Fibrillation • Calcium Transient

SECTION A SINGLE CELL ACTION POTENTIALS

1.	Introduction	1
1.1.	Heart Structure and Conduction Pathways	1
1.2.	Membrane Potential	1
1.3.	Ion Channels	2
1.4.	Formation of the Action Potential.....	4
2.	Computer Modelling Methods.....	6
3.	Results.....	6
3.1.	Bachmann's Bundle	6
3.1.1	Transient Outward Potassium Current.....	6
3.1.2	L-type Inward Calcium Current.....	7
3.1.3	Action Potential.....	8
3.2.	Coronary Sinus.....	9
3.2.1	Transient Outward Potassium Current.....	9
3.2.2	L-type Inward Calcium Current.....	10
3.2.3	Action Potential.....	11
3.3.	Pulmonary Vein	11
3.3.1	Transient Outward Potassium Current.....	11
3.3.2	L-type Inward Calcium Current.....	12
3.3.3	T-type Inward Calcium Current	13
3.3.4	Rapid Delayed Rectifier Potassium Current.....	14
3.3.5	Inward Rectifier Potassium Current	15
3.1.3	Action Potential.....	16
4.	Discussion	16
4.1	Restitution Curves	16

SECTION B SPONTANEOUS ACTION POTENTIALS AND ATRIAL FIBRILLATION

1.	Introduction	17
1.1.	Receptor Gated Ion Channels and Calcium Dynamics.....	17
1.2.	Calcium Activated Currents	18
1.3.	Initiation of Normal Pacemaker Activity.....	18
2.	Computer Modelling Methods.....	18
3.	Results.....	18
3.1.	Hyperpolarising Activated Current	18
3.2.	Calcium Activated Currents	18
3.3.	Sustained Spontaneous Activity	19
4.	Discussion	19
	Acknowledgements	20
	References	20

A. ACTION POTENTIAL MODELS

1. Introduction

Heart disease is the single most common cause of death in western society and so there is great importance placed on understanding heart function and the origin of dangerous variations in sinus rhythm such as arrhythmia and tachycardia. Voltage-clamp techniques have been used for many years to probe the electrophysiology of single cardiomyocytes as well as tissue with a view to assembling a complete picture of how the heart functions. Data from these experiments can be used to develop computer models of cardiomyocyte behaviour which can then be used to simulate the effect of any number of physical factors, including response to drugs. A complete model of cardiac electrophysiology would provide pharmacologists with a powerful tool for drug development and testing.

1.1. Heart Structure and Conduction Pathways

The heart is a muscular structure with four chambers (*Figure 1*). Its primary function is to facilitate the supply of oxygenated blood to muscle groups and organs throughout the body. The heart receives blood from the veins at low pressure, raises the pressure by contracting rhythmically around the blood, and then ejects it into the arterial system at this higher pressure.

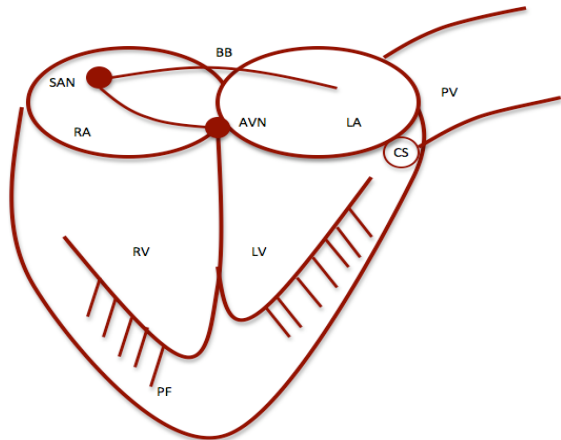


Figure 1: Schematic of the human heart showing the four chambers and main conduction pathways.

RA: Right Atrium

LA: Left Atrium

RV: Right Ventrical

LV: Left Ventrical

SAN: Sinoatrial node

AVN: Atrioventricular node

BB: Bachmann's Bundle

PV: Pulmonary Vein

CS: Coronary Sinus

PF: Purkinje Fibres

(Adapted from Sakamoto 2005)

Contraction and relaxation of cardiac muscles, and therefore sinus rhythm, have an electrophysiological basis. An electrical impulse known as an action potential, AP, generated in the pace-making cells of the sinoatrial node propagates through the heart via cell-to-cell conduction. A cell depolarises, allowing positive charge to accumulate inside the sarcolemma. Ionic currents can flow to adjoining cells, if this intercellular current is high enough to depolarise these adjacent cells an AP is generated. This electrical activity causes muscular contraction. (Klabunde 2005)

In order for the heart to effectively increase the pressure of incoming blood and maintain correct blood flow direction, it must contract in a very specific way. To achieve this, the AP generated in the SA node travel through the atria, causing them to contract first, before passing to the atrioventricular node. After a pause, the AP is conducted through the bundle of His to the Purkinje fibers. This ordering of the conduction system allows for almost perfectly synchronous contraction of the ventricular myocytes. In this paper we concern ourselves with interatrial conduction. (Klabunde 2005)

A specialised pathway for interatrial conduction was first suggested by Bachmann in 1916. It has since been shown that Bachmann's bundle is the primary interatrial conduction pathway, and that the coronary sinus is secondary in this function. The preferred pathway changes depending on the site of excitation, with distance from the pacing site to proximal end of the pathway being the primary deciding factor. (Sakamoto 2005) As is seen in *Figure 1* Bachmann's bundle, originates inside the sinoatrial node, and so this is the preferred pathway in normal sinus rhythm. The pulmonary vein does not act as an interatrial conduction pathway, but it has been shown to act as an ectopic pacemaker, which can alter the preferred pathway and may be the cause of atrial fibrillation. (Honjo 2003) We consider it here for use in Section B of this report.

1.2. Membrane Potential

Changes of the membrane potential during the AP are due to flows of different ions across the cell membrane. The cell membrane can be thought of as a set of parallel electrical circuits (*Figure 2*), where each ion is a voltage source in series with a variable resistance. The voltage source is the ions equilibrium potential, E_{ion} , and the resistance is

the reciprocal of the ions conductance, $1/g_{ion}$. The equilibrium potential for any ion can be calculated using the Nernst equation;

$$E_{ion} = \frac{RT}{zF} \ln \frac{[ion]_o}{[ion]_i}, \quad (1)$$

where R is the gas constant, T the absolute temperature, z the charge on the ion, F the Faraday constant, and $[ion]_o$ and $[ion]_i$ are the intracellular and extracellular ion concentrations respectively. The resting membrane potential, E_R , of any cardiomyocyte can then be written as;

$$E_R = \frac{\sum g_{ion} E_{ion}}{\sum g_{ion}}, \quad (2)$$

where E_R is the RP. In the resting state, the membrane is highly permeable to potassium ions and only slightly permeable to other ions, this means that for most cardiomyocytes, E_R is very close to E_{K^+} . (Klabunde 2005)

Stimulating a cell electrically alters the membrane potential. The difference between this new potential, V_m , and E_{ion} generates ionic currents with a general form given by;

$$I_{ion} = g_{ion} (V_m - E_{ion}). \quad (3)$$

By convention, the influx of negative ions or the efflux of positive ions is called an outward current. Conversely, the influx of positive ions and the efflux of negative ions is called an inward current. (Guevara 1991)

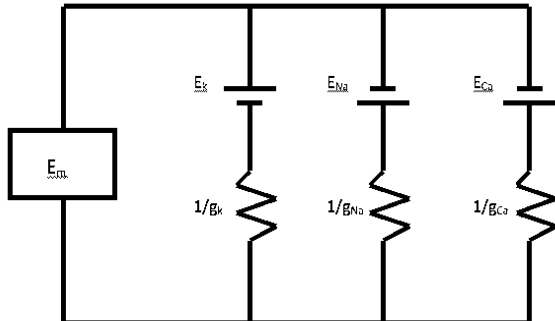


Figure 2: The cell membrane as a parallel circuit.

Each ion is a voltage source in series with a variable resistance

(Adapted from Klabunde 2005)

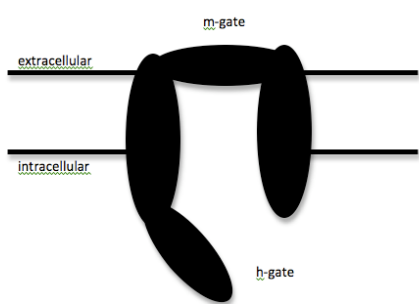
In order for this model to function, ionic concentration gradients must be maintained across the membrane, an active process that requires the use of energy. The concentration gradients of potassium and sodium lead to a situation where sodium leaks into the cell when it is at rest and potassium leaks out. During AP, more potassium leaves the cell and more sodium enters. Although the number of ions involved in these transfers is small compared to the total number of ions available, many successive APs can alter the concentration gradients significantly. This is prevented by the action of the sodium-potassium adenosine triphosphatase pump, which removes sodium from the cell and introduces potassium.

Calcium concentrations are maintained in a similar fashion. The ATP dependent calcium pump removes calcium from the cell, and the sodium-calcium exchanger, I_{NaCa} , exchanges three sodium ions for two calcium ions across the membrane and can operate in either direction depending on the membrane potential. (Klabunde 2005) The sodium-calcium exchanger plays a role in spontaneous activity in the pulmonary vein and will be considered in more detail in Section B.

1.3. Ion Channels

Various ions pass through specific channels in the cell membrane. These channels are specific in that each type of channel allows only one type of ion to pass. A specific ion channel consists of two trans-membrane proteins gated at each end. The m-gate is at the outside edge of the channel and the h-gate is at the inside edge (Figure 3).

Two types exist, channels to voltage that in this first section we consider only voltage gated channels.



of

Figure 3. Ion channel in its resting state.

Though the h-gate is open, the m gate is closed so no ion transfer occurs.

(Adapted from Katz 2001)

ion channels voltage gated that respond changes in across the cell membrane and receptor gated channels respond to chemical signals. (Klabunde 2005) In this

These two gates allow the channel to have three separate states as described by the Hodgkin-Huxley model, summarised in Table 1. From an initial resting state, a voltage stimulus activates the channel, opening the m-gate and allowing ion transfer. The channel is now in the open state, during this time a change in potential across the membrane takes the channel into a period of refractory where it is unresponsive to voltage stimuli and the probability of the channel closing increases. The channel moves to the closed state as the h-gate closes and in order to reactivate the channel another voltage stimulus is needed. This cycle is depicted in Figure 4.

Table 1: Summary of the two-gate Hodgkin-Huxley model

State	m-gate	h-gate
Resting	Closed	Open
Open	Open	Open
Closed	Open	Closed

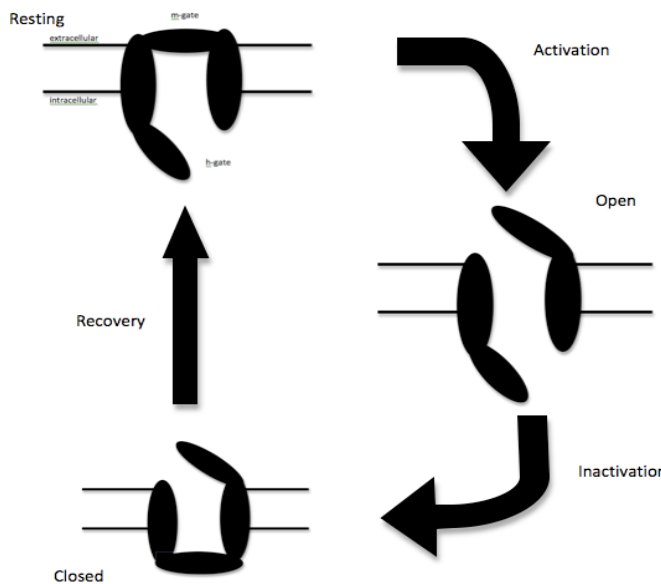


Figure 4: The Hodgkin-Huxley model of ion channel activity.

Shows the three states and the processes by which a single channel moves between them

(Adapted from Katz 2001)

The voltage stimuli referred to above are in fact changes in polarization of the cell membrane. In the specific case of cardiac cells, sodium and calcium ions pass through when their channels are open, this depolarises the membrane until a voltage is reached at which the potassium channels open and potassium flows out of the cell, repolarising the cell membrane. After repolarisation, during recovery, the sodium and calcium channels reactivate, causing a transition back to the resting state where the m-gate closes and the h-gate opens. (Katz 2001)

The processes of activation and inactivation are time dependent, governed by the activation and inactivation variables, r and s respectively. These variables are different for each specific ion channel but have a general form, which we derive here. We assume, for any specific ion channel, that the fraction of open gates at any one time is r and that the fraction of closed gates is $(1 - r)$. This leads us to the first order differential equation that r must satisfy;

$$\frac{dr}{dt} = \alpha(1 - r) - \beta r, \quad (4)$$

where; α is the rate of gate opening and β is the rate of closing. When $r = 1$ all channels are open and the current is fully active, when $r = 0$ all channels are closed and the current is fully inactive. We rewrite this as;

$$\frac{dr}{dt} = \frac{(\bar{r} - r)}{\tau_r}, \quad (5)$$

where the steady-state value, \bar{r} is;

$$\bar{r} = \frac{\alpha}{\alpha + \beta}, \quad (6)$$

and the time constant of activation, τ_r is;

$$\tau_r = \frac{1}{\alpha + \beta}, \quad (7)$$

If V_m is held constant then the solution to (5) can be written as;

$$\bar{r} = r_0 + (\bar{r} - r_0) \exp(-t/\tau_r), \quad (8)$$

where $r_0 = r(t=0)$. A similar set of expressions exist for inactivation, but not all of the specific ion channels experience this. It is possible for a single specific ion channel to have several activation or inactivation variables (see section 1.3). The expressions derived above can be used to find the ion current associated with a specific ion channel and its set of variables as an extension to the general form shown in equation (3).

$$I_{ion} = g_{ion} r_{ion}^\lambda s_{ion}^{\lambda} (V_m - E_{ion}), \quad (9)$$

where λ is the number of gates. (Guevara 1991)

1.4. Formation of the Action Potential

Ion channels exist in groups, for example, in Bachmann Bundle (BB) cells there are two calcium channels and several different potassium channels. These channels are differentiated from each other by their activation and inactivation variables and their time constants. *Figure 5* shows the ionic currents typically found in cardiac cells, not all currents are found in all cell types. The total current flowing across the cell membrane at any time is the sum of individual specific ion channel currents.

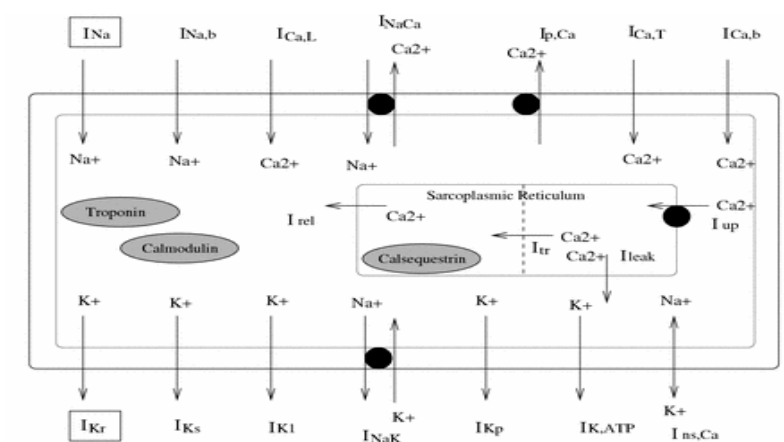


Figure 5: Transmembrane Ionic Channels within cell structure.

The sarcoplasmic reticulum is an organelle that contains a store of calcium

(Lloyd 2001)

The cell membrane is effectively two electrolytic solutions separated by a dielectric layer of phospholipid, a capacitor. We can apply the usual equations to describe capacitor behaviour including;

$$\frac{dV}{dt} = -\sum_{ion} I_{ion} / C_m, \quad (10)$$

where C_m is the cell capacitance and I_{ion} are the various ionic currents as described in (). During resting, most currents are inactive. When a stimulus is applied ion transfer begins, I_{ion} becomes non-zero and an AP is generated. (Guevara 1991) The general atrial AP comprises five phases (Figure 6).

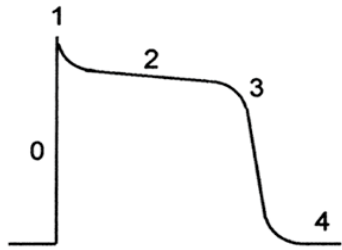


Figure 6: A general atrial action potential showing the 5 phases.

(Medscape 2003)

Phase 0 is a rapid depolarisation to around +20mV, initiated by the opening of sodium channels allowing the fast current, I_{Na} , to bring Na^+ ions into the cell. I_{Na} activation and inactivation are fast processes so this phase is over quickly.

Phase 1 is an initial repolarisation to around 0mV as a result of the transient outward current, I_{to} , potassium current to flow into the cell.

Phase 2 is a plateau at constant potential. The L-type, I_{CaL} , and T-type, I_{CaT} , calcium currents, and to a lesser degree I_{Na} , bring positive ions into the cell, countering the repolarisation effect of I_{to} . I_{CaL} initiates calcium release from the sarcoplasmic reticulum, SERCA, which further counters repolarisation.

Phase 3 is a second stage of repolarisation to the RP. The slow and fast delayed rectifying potassium currents, I_{Ks} and I_{Kr} respectively, which have longer activations than I_{to} , become functional and bring potassium out of the cell.

Phase 4 is the resting phase. The RP is determined by the inward rectifying potassium current, I_{K1} , which is fully active in this phase as opposed to the sodium and calcium channels which are in recovery. (Katz 2001)

Phases 0-3 are known as the effective refractory period (ERP). During this time all h-gates are closed and no new AP can be generated, no matter how high the stimulation. This is a protective mechanism that keeps AP frequency, and therefore heart rate, within a safe upper limit. Phases 3-4 are known as the relative refractory period (RRP). During this time only a few h-gates are open and so an unusually high stimulus is required to initiate a new AP. These concepts are demonstrated in Figure 7. (Klabunde 2005)

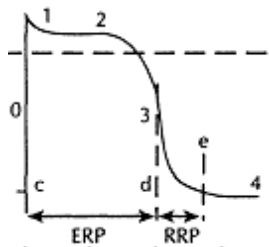


Figure 7: The effective and relative refractory periods of a general atrial action potential.

(Berne 1999)

The AP has a distinct form depending on which type of myocyte it is associated with, but all have common features that can provide insight into the underlying ion kinetics. We have referred to the RP in Section 1.2. It is the potential difference across the cell membrane when the cell is at rest and is therefore the baseline from which an AP deviates. The RP is largely set by the equilibrium potential of potassium, its value can tell us about the potassium currents as well as the strength of the exchangers and pumps that regulate concentrations. The maximum deviation from the RP during AP is the AP amplitude, APA. The AP duration, APD, varies significantly between cell types. It is dependent on the ability of the potassium currents to repolarise the cell, stronger potassium currents mean that repolarisation occurs more quickly, leading to a shorter APD. APD is also dependent on the frequency of stimulation, the inverse of the basic cycle length (BCL), unless the AP is in the RRP or a later phase, no stimulus of any strength can initiate a successive AP. APD is short when BCL is short, and longer when BCL increases. (Katz 2001) APD in this paper refers specifically to APD₉₀, the time taken for the cell to return to 90% of its maximum polarisation.

2. Computer Modelling Methods

The main goal of this work was to develop a mathematical model of the rabbit cardiomyocytes that comprise the main interatrial conduction pathways and the pulmonary vein, based on single-cell voltage clamp data. Data was not available for all currents which has limited our models, in particular that of the coronary sinus where there was no experimental AP against which to compare our final model.

Using ScanIt we were able to extract current-voltage relationships, steady-state activation/inactivation curves and time constants from published experimental figures. The resultant data was used to construct computer codes for individual ionic currents: using an existing model of a rabbit atrial myocyte as a basis, parameters of each code were changed in order to produce current characteristics fitting to the collected experimental data. The single current codes were combined into a single-cell model were simulate the complete AP. The computation is carried out at small time-steps HT that can be defined to prevent rapidly changing variables from crashing the program.

The general expression used for steady-state activation and inactivation is;

$$\bar{r} = \frac{1}{1 + e^{-(V_m - V_{0.5})/K}}, \quad (11)$$

where $V_{0.5}$ is the membrane potential at half-activation/inactivation and K is the gradient of the slope at $V_m = V_{0.5}$.

3. Results

The programs we created are able to output the membrane potential at each time-step and any other currents or ion concentrations one chooses. As such the data can be represented graphically to fully understand the processes involved during stimulation. Powerful computer spreadsheet software with a graphical data toolkit was used to produce the succeeding panels for each single-current code in the three cell types.

Each panel comprises: the current-voltage relationship and its current trace at each stage of the voltage-clamp protocol and where appropriate for the voltage and time-dependent ion channels the activation-inactivation curves and time constants.

3.1. Bachmann's Bundle

3.1.1. Transient outward potassium current, I_{to}

I_{to} kinetics are described by one activation variable (r), three inactivation variables (s_1 , s_2 and s_3 ; the fast, slow and third respectively), and their corresponding time constants (τ_r , τ_{s1} , τ_{s2} and τ_{s3}). The activation and inactivation variables that fit with experimental data from Boyden (2007) are expressed as;

$$r = \frac{1}{\left(1 + \exp\left(-\frac{(V+15)}{5.633}\right)\right)}, \quad (12)$$

$$s_1 = \frac{1}{\left(1 + \exp\left(\frac{(V+28)}{5.3}\right)\right)}, \quad s_2 = \frac{1}{\left(1 + \exp\left(\frac{(V+28)}{5.3}\right)\right)} \text{ and } s_3 = \frac{1.666}{\left(1 + \exp\left(\frac{(V+50.67)}{27.38}\right)\right)} + 0.4, \quad (13,14,15)$$

Time constants taken from the online supplement to the same paper are expressed as;

$$\tau_r = \frac{1}{386.6 \times \left(\exp\left(\frac{V}{12}\right)\right) + 8.011 \times \left(\exp\left(\frac{-V}{7.2}\right)\right)} + 0.0004, \quad (16)$$

$$\tau_{s1} = \frac{0.1199}{\left(1 + \exp\left(\frac{(V+32.8)}{0.1}\right)\right)} + 0.0157, \quad \tau_{s2} = \frac{3.161}{\left(1 + \exp\left(\frac{(V+32.8)}{0.1}\right)\right)} + 0.1103 \text{ and} \quad (17,18)$$

$$\tau_{s3} = \frac{7.5}{\left(1 + \exp\left(\frac{(V+23)}{0.5}\right)\right)} + 0.5 \quad (19)$$

The I_{to} current trace could then be produced using the newly modified equation;

$$I_{to} = 27.0108 \times r \times ((0.59 \times s_1^3) + (0.41 \times s_2^3)) \times ((0.6 \times s_3^6) + 0.4) \times (V - E_K), \quad (20)$$

Putting all this together gives us the following relationships (Figure 8);

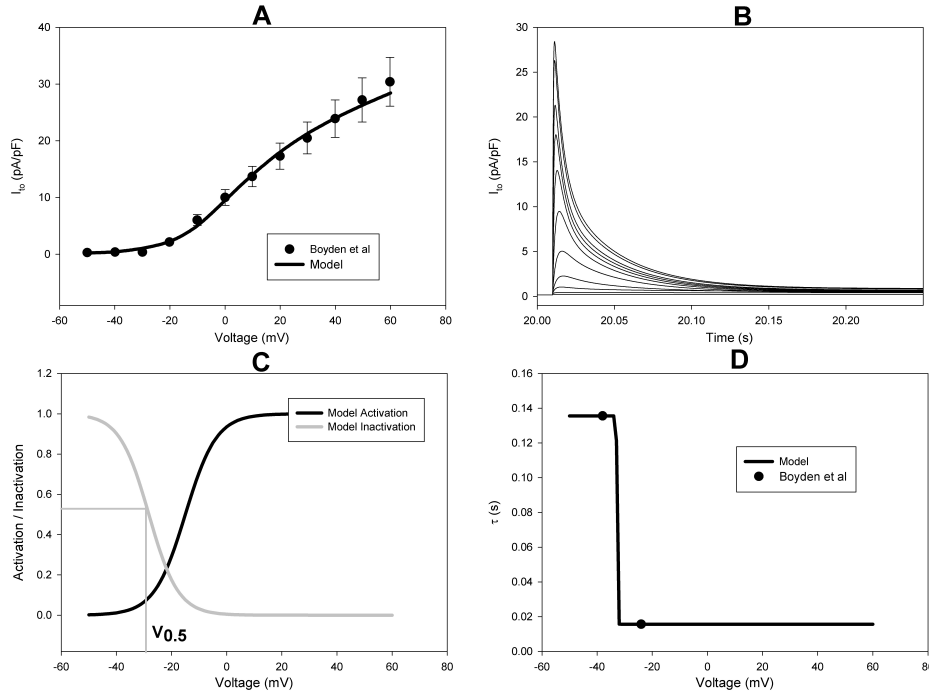


Figure 8: A) Current-Voltage curve for I_{to} in Bachmann's Bundle; B) Current traces for isolated cells from a holding potential of -60 mV with 10 mV depolarising steps to voltages from -50 to +60 mV; C) Activation-Inactivation curves and D) time constant

3.1.2. L-type inward calcium Current, I_{CaL}

I_{CaL} kinetics are described by one activation variable (r), and one inactivation variable (s) and their corresponding time constants (τ_r , τ_1 , τ_2). The activation and inactivation variables that fit with experimental data from Boyden (2007) are expressed as;

$$r = \frac{1}{\left(1 + \exp\left(-\frac{(V - 7.9)}{6.3}\right)\right)}, \quad (21)$$

$$s = \frac{1}{\left(1 + \exp\left(\frac{(V + 20.4)}{6.3}\right)\right)}, \quad (22)$$

Time constants taken from the online supplement to the same paper are expressed as;

$$\tau_r = \left(\frac{\exp(-(V + 45)/2.5) - 1}{-16.72 \times (V + 45)} - \frac{\exp(-(V - 10)/4.808) - 1}{50 \times (V + 10)} \right) + \left(\frac{\exp((V + 5)/2.5) - 1}{4.48 \times (V + 5)} \right), \quad (23)$$

$$\tau_1 = \frac{0.0291}{\left(1 + \exp\left(\frac{(V + 18)}{4}\right)\right)} + 0.0132, \quad \tau_2 = \frac{2.1654}{\left(1 + \exp\left(\frac{(V + 18)}{4}\right)\right)} + 0.0506, \quad (24, 25)$$

The I_{CaL} current trace could then be produced using the newly modified equation for this current;

$$I_{CaL} = 16 \times r \times s \times (V - 61.4), \quad (26)$$

Putting all this together gives us the following relationships (Figure 9);

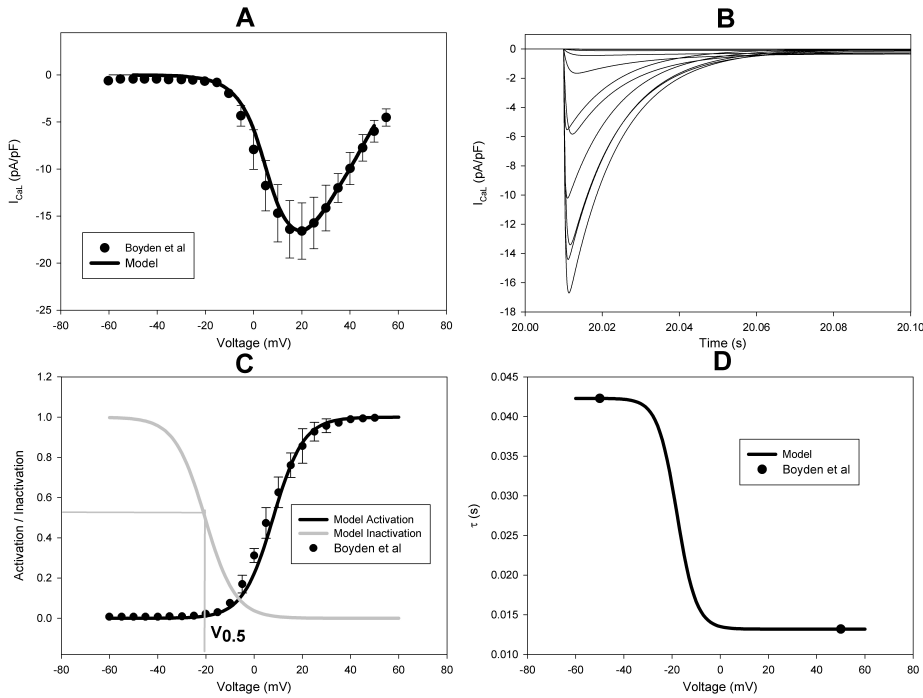


Figure 9: A) Current-Voltage curve for I_{Cal} in Bachmann's Bundle; B) Current traces for isolated cells from a holding potential of -70 mV to voltages from -60 to +55 mV; C) Activation-Inactivation curves and D) time constant

3.1.3. Action Potential

Individual currents for BB were combined in the whole cell model. The model includes a sustained outward current comprising potassium and chloride background currents that can be seen to significantly effect the APD. This current was included in our code and altered until our modelled AP agreed well with that found experimentally by Boyden (2007).

$$I_{\text{sus}} = 0.3 \times (V + 85), \quad (27)$$

Another current for which there was no experimental data but which nonetheless effects the AP significantly is I_{K1} . It was altered to get an RP which agreed with Boyden (2007) and expressed as;

$$I_{K1} = \frac{2.955 \times (V - E_K - 12)}{\left(1 + \exp\left(\frac{1.393 \times F}{RT} \times (V - E_K - 12)\right)\right) + 0.05}, \quad (28)$$

The final AP simulated at BCL=400ms is shown below (Figure 10).

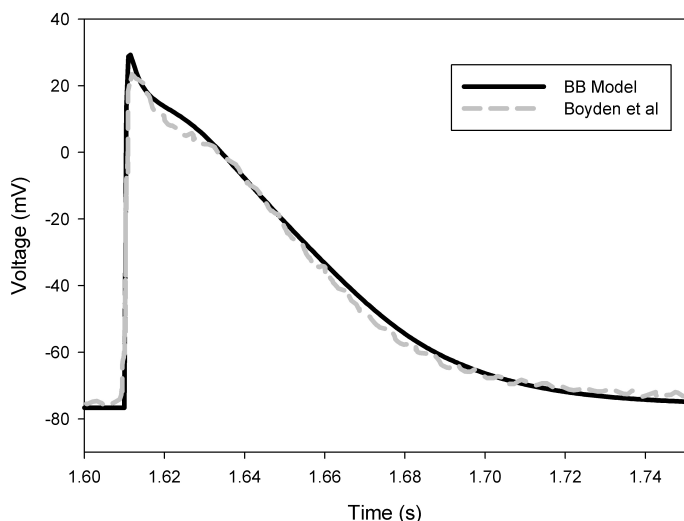


Figure 10: The simulated (solid) and recorded (dashed) action potentials for BB cells in rabbit atria. Resting potential -76 mV, APD 88 ms and APA 100mV with BCL 400 ms (c.f. Boyden et al. Resting potential -76 mV, APD 90 ms and APA 100 mV)

3.2. Coronary Sinus

3.2.1. Transient outward potassium current, I_{to}

I_{to} kinetics are described by one activation variable (r), three inactivation variables (s_1 , s_2 and s_3 ; the fast, slow and third respectively), and their corresponding time constants (τ_r , τ_{s1} , τ_{s2} and τ_{s3}). The activation and inactivation variables that fit with experimental data from Boyden (2007) are expressed as;

$$r = \frac{1}{\left(1 + \exp\left(-\frac{(V+15)}{5.633}\right)\right)}, \quad (29)$$

$$s_1 = \frac{1}{\left(1 + \exp\left(\frac{(V+24.8)}{5.6}\right)\right)}, \quad s_2 = \frac{1}{\left(1 + \exp\left(\frac{(V+248)}{5.6}\right)\right)} \quad \text{and} \quad s_3 = \frac{1.666}{\left(1 + \exp\left(\frac{(V+50.67)}{27.38}\right)\right)} + 0.4, \quad (30,31,32)$$

Time constants taken from the online supplement to the same paper are expressed as;

$$\tau_r = \frac{1}{386.6 \times \left(\exp\left(\frac{V}{12}\right) + 8.011 \times \left(\exp\left(\frac{-V}{7.2}\right)\right)\right) + 0.0004}, \quad (33)$$

$$\tau_{s_1} = \frac{0.0496}{\left(1 + \exp\left(\frac{(V+32.8)}{0.1}\right)\right)} + 0.0158, \quad \tau_{s_2} = \frac{2.9536}{\left(1 + \exp\left(\frac{(V+32.8)}{0.1}\right)\right)} + 0.1245 \quad \text{and} \quad (34,35)$$

$$\tau_{s_3} = \frac{7.5}{\left(1 + \exp\left(\frac{(V+23)}{0.5}\right)\right)} + 0.5, \quad (36)$$

The I_{to} current trace could then be produced using the newly modified equation;

$$I_{to} = 15.5062 \times r \times ((0.59 \times s_1^3) + (0.41 \times s_2^3)) \times ((0.6 \times s_3^6) + 0.4) \times (V - E_K), \quad (37)$$

Putting all this together gives us the following relationships (Figure 11);

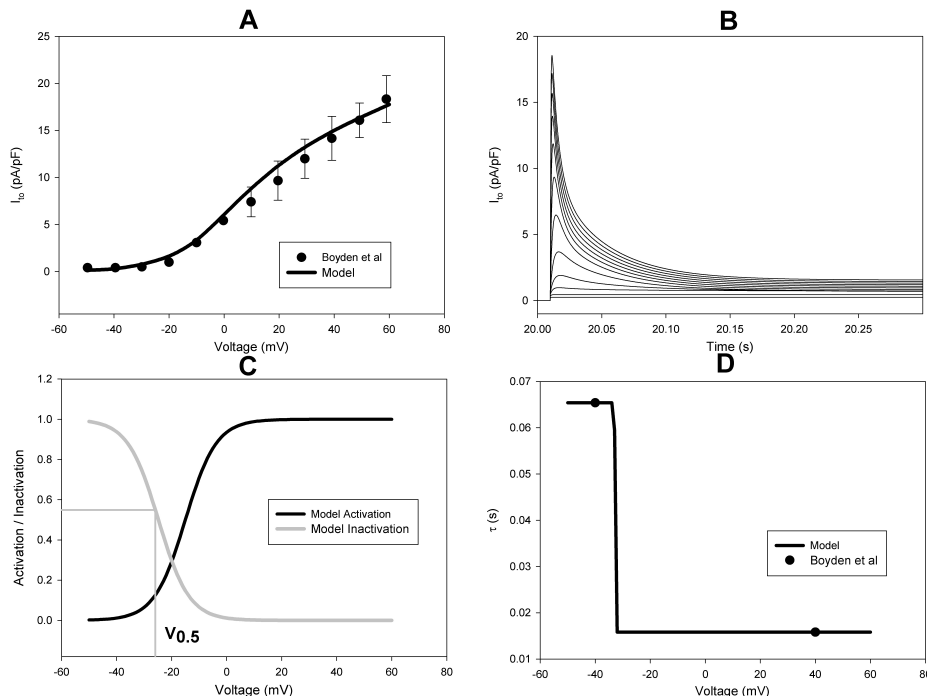


Figure 11: A) Current-Voltage curve for I_{to} in the Coronary sinus; B) Current traces for isolated cells from a holding potential of -60 mV with 10 mV depolarising steps to voltages from -50 to +60 mV; C) Activation-Inactivation curves and D)time constant

3.2.2. L-type inward calcium Current, I_{CaL}

I_{CaL} kinetics are described by one activation variable (r), one inactivation variables (s) and their corresponding time constants (τ_r , τ_1 , τ_2). The activation and inactivation variables that fit with experimental data from Boyden (2007) are expressed as;

$$r = \frac{1}{\left(1 + \exp\left(-\frac{(V - 0.5)}{5.7}\right)\right)}, \quad (38)$$

$$s = \frac{1}{\left(1 + \exp\left(\frac{(V + 17.9)}{5.2}\right)\right)}, \quad (39)$$

Time constants taken from the online supplement to the same paper are expressed as;

$$\tau_r = \left(\frac{\exp(-(V + 45)/2.5) - 1}{-16.72 \times (V + 45)} - \frac{\exp(-(V - 10)/4.808) - 1}{50 \times (V + 10)} \right) + \left(\frac{\exp((V + 5)/2.5) - 1}{4.48 \times (V + 5)} \right), \quad (40)$$

$$\tau_1 = \frac{0.0335}{\left(1 + \exp\left(\frac{(V + 18)}{4}\right)\right)} + 0.0117, \quad \tau_2 = \frac{2.2989}{\left(1 + \exp\left(\frac{(V + 18)}{4}\right)\right)} + 0.0478, \quad (41)$$

The I_{CaL} current trace could then be produced using the newly modified equation for this current;

$$I_{CaL} = 28.8 \times r \times (0.8 \times s[\tau_1] + 0.2 \times s[\tau_2]) \times (V - 58.3), \quad (42)$$

Putting all this together gives us the following relationships (Figure 12);

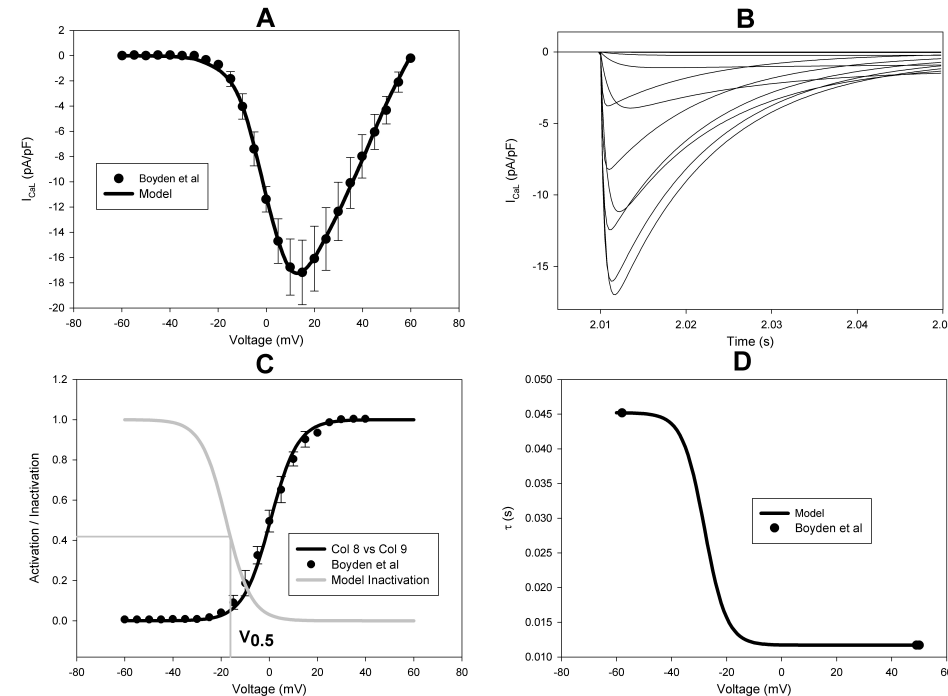


Figure 12: A) Current-Voltage curve for I_{CaL} in the Coronary Sinus; B) Current traces for isolated cells from a holding potential of -70 mV to voltages from -60 to +55 mV; C) Activation-Inactivation curves and D) time constant

3.2.3. Action Potential

Individual currents for CS were combined in the whole cell model. Since there exists no data against which to compare our simulated AP, the sustained outward current was included unaltered from the original model.

$$I_{sus} = 0.4 \times (V + 85) + 0.2 \times (V - 5), \quad (43)$$

where the first term is the K^+ current and the second term the Cl^- current. I_{K1} was also included unaltered as;

$$I_{K1} = \frac{3.635 \times (V - E_K - 12)}{\left(1 + \exp\left(\frac{1.393 \times F}{RT} \times (V - E_K - 12)\right)\right) + 0.05}, \quad (44)$$

The final AP simulated at BCL=400ms is shown below (Figure 13).

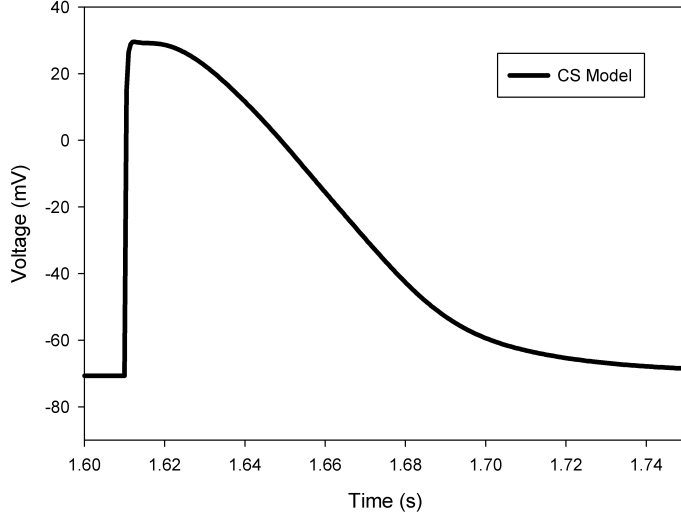


Figure 13: The simulated action potential for the coronary sinus. Resting potential -76 mV, APD 91.2 mV and APA 100 mV.

3.3. Pulmonary Vein

3.3.1. Transient outward potassium current, I_{to}

I_{to} kinetics are described by one activation variable (r), two inactivation variables (s_1, s_2 ; the fast, slow respectively), and their corresponding time constants ($\tau_r, \tau_{s1}, \tau_{s2}$). The activation and inactivation variables that fit with experimental data from Boyden (2007) are expressed as;

$$r = \frac{1}{\left(1 + \exp\left(-\frac{(V+15)}{5.633}\right)\right)}, \quad (45)$$

$$s_1 = \frac{1}{\left(1 + \exp\left(\frac{(V+28)}{5.3}\right)\right)}, \quad s_2 = \frac{1}{\left(1 + \exp\left(\frac{(V+29.4)}{5.1}\right)\right)} \text{ and } s_3 = \frac{1.666}{\left(1 + \exp\left(\frac{(V+50.67)}{27.38}\right)\right)} + 0.4, \quad (46,47,48)$$

Time constants taken from the online supplement to the same paper are expressed as;

$$\tau_r = \frac{1}{386.6 \times \left(\exp\left(\frac{V}{12}\right)\right) + 8.011 \times \left(\exp\left(\frac{-V}{7.2}\right)\right)} + 0.0004, \quad (49)$$

$$\tau_{s_1} = \frac{0.1155}{\left(1 + \exp\left(\frac{(V+32.8)}{0.1}\right)\right)} + 0.0147, \quad \tau_{s_2} = \frac{3.0967}{\left(1 + \exp\left(\frac{(V+32.8)}{0.1}\right)\right)} + 0.0926 \text{ and} \quad (50,51)$$

$$\tau_{s_3} = \frac{7.5}{\left(1 + \exp\left(\frac{(V+23)}{0.5}\right)\right)} + 0.5 \quad (52)$$

The I_{to} current trace could then be produced using the newly modified equation for this current;

$$I_{to} = 11.5921 \times r \times \left((0.8 \times s_1^3) + (0.2 \times s_2^3) \right) \times (V - E_K), \quad (53)$$

Putting all this together gives us the following relationships (Figure 14);

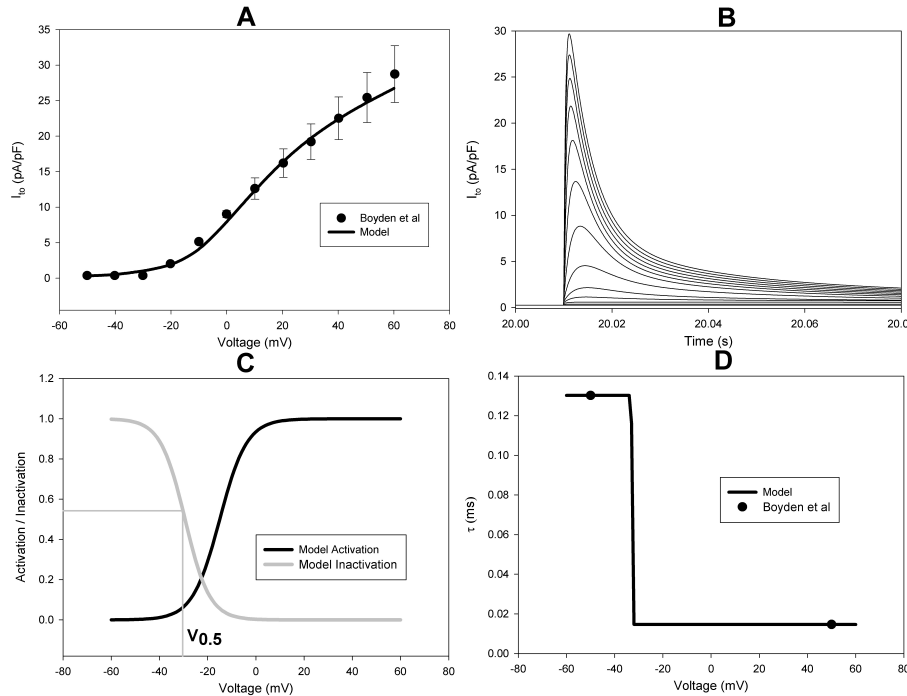


Figure 14: A) Current-Voltage curve for I_{CaL} in the coronary sinus. B) Current traces for isolated cells from a holding potential of -60 mV with 10 mV depolarising steps to voltages from -50 to +60 mV; C) Activation-Inactivation curves and D) time constant

3.3.2. L-type inward calcium current, I_{CaL}

I_{CaL} kinetics are described by one activation variable (r), one inactivation variable (s), and their corresponding time constants (τ_r , τ_1 , τ_2). The activation and inactivation variables that fit with experimental data from Boyden (2007) are expressed as;

$$r = \frac{1}{1 + \exp\left(-\frac{(V + 7.5)}{5.5}\right)}, \quad (54)$$

$$s = \frac{1}{1 + \exp\left(\frac{(V + 23.4)}{5.2}\right)}, \quad (55)$$

Time constants taken from the online supplement to the same paper are expressed as;

$$\tau_r = \left(\frac{\exp(-(V + 45)/2.5) - 1}{-16.72 \times (V + 45)} - \frac{\exp(-(V - 10)/4.808) - 1}{50 \times (V + 10)} \right) + \left(\frac{\exp((V + 5)/2.5) - 1}{4.48 \times (V + 5)} \right), \quad (56)$$

$$\tau_1 = \frac{0.0336}{1 + \exp\left(\frac{(V + 18)}{4}\right)} + 0.0142, \quad \tau_2 = \frac{3.6908}{1 + \exp\left(\frac{(V + 18)}{4}\right)} + 0.0534, \quad (57, 58)$$

The I_{CaL} current trace could then be produced for different membrane potentials using the newly modified equation for this current;

$$I_{CaL} = 25 \times r \times s \times (V - 58.3), \quad (59)$$

Putting all this together gives us the following relationships (Figure 15);

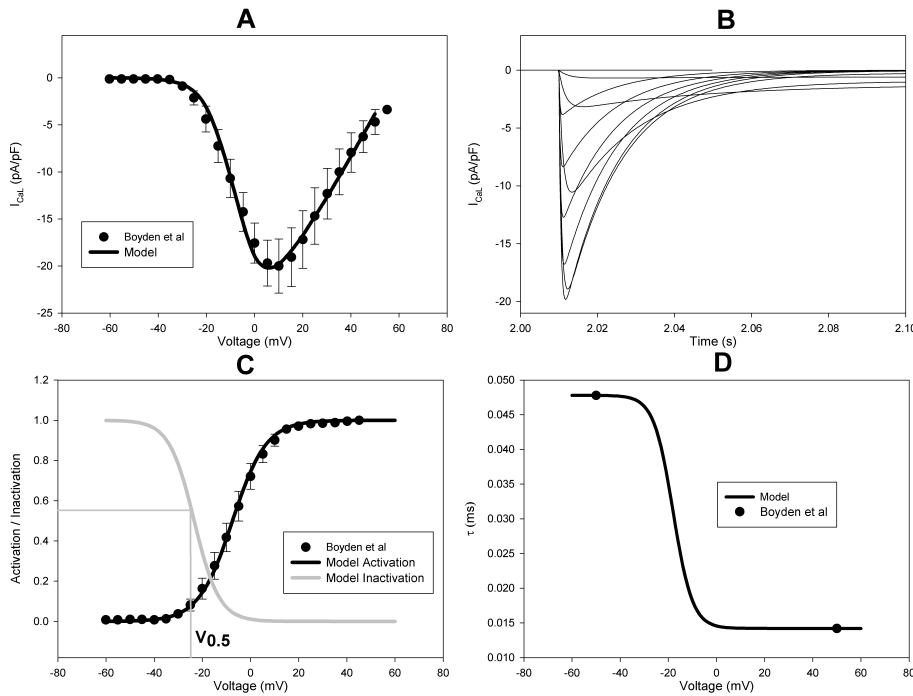


Figure 15: A) Current-Voltage curve for I_{CaL} in the pulmonary vein; B) Current traces for isolated cells from a holding potential of -70 mV to voltages from -60 to +55 mV; C) Activation-Inactivation curves and D) time constant

3.3.3. T-type inward calcium current, I_{CaT}

I_{CaT} kinetics are described by one activation variable (r), one inactivation variable (s), and their corresponding time constants (τ_r , τ_s). The activation and inactivation variables that were modelled based on data from Chen (2004) are expressed as;

$$r = \frac{1}{1 + \exp\left(-\frac{(V + 23)}{5.1}\right)}, \quad (60)$$

$$s = \frac{\exp\left(-\frac{(V + 94)}{83.3}\right)}{\left(\exp\left(-\frac{(V + 94)}{83.3}\right) + \exp\left(\frac{(V + 94)}{16.3}\right)\right)}, \quad (61)$$

Time constants, also modelled based on this data, are expressed as;

$$\tau_r = \frac{1}{9674.173 \times \left(\exp\left(\frac{(V + 23.3)}{30}\right) + \exp\left(-\frac{(V + 23.3)}{30.0}\right)\right)}, \quad (62)$$

$$\tau_s = \frac{1}{9.637 \times \left(\exp\left(-\frac{(V + 94)}{83.3}\right) + \exp\left(\frac{(V + 94)}{16.3}\right)\right)}, \quad (63)$$

The I_{CaT} current trace could then be produced for different membrane potentials using the newly modified equation for this current;

$$I_{CaT} = 13.2 \times r \times s \times (V - 38), \quad (64)$$

Putting all this together gives us the following relationships (Figure 16);

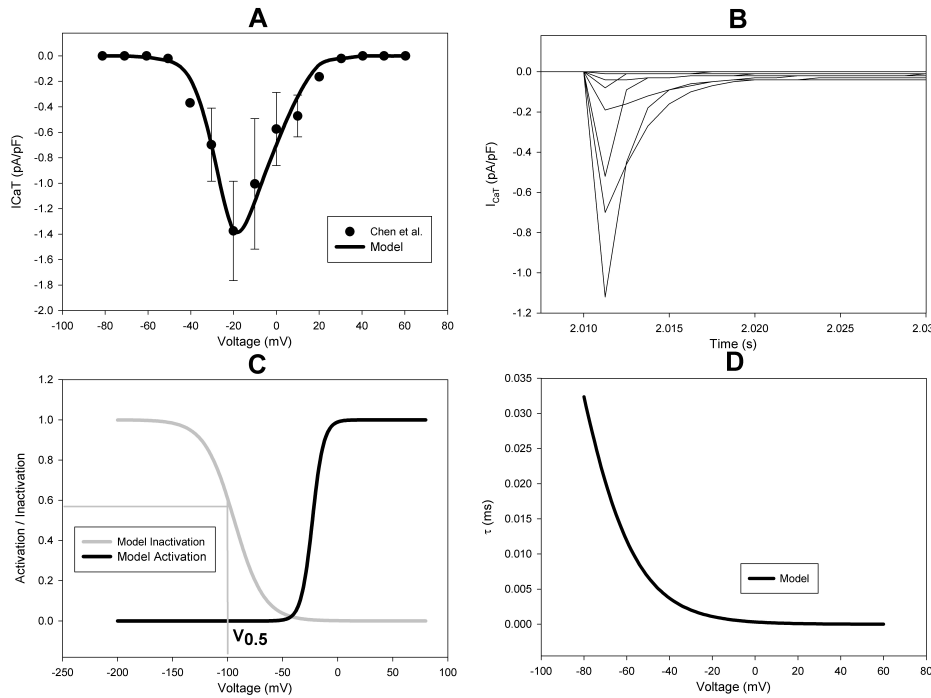


Figure 16: A) Current-Voltage curve for I_{CaT} in the pulmonary vein; B) Current traces for isolated cells from a holding potential of -40 mV with 10 mV depolarising steps to voltages from -80 to +60 mV; C) Activation-Inactivation curves and D) time constant

3.3.4. Rapid delayed rectifier potassium current, I_{Kr}

I_{Kr} kinetics are described by one activation variable (r), one inactivation variable (s_1), and their corresponding time constants (τ_r , τ_s). The activation and inactivation variables that were modelled based on data from Earm (2008) are expressed as;

$$r = \frac{1}{1 + \exp\left(-\frac{(V + 5.1)}{7.4}\right)}, \quad (65)$$

$$s = \frac{1}{1 + \exp\left(\frac{(V + 47.3921)}{18.6603}\right)}, \quad (66)$$

Time constants, also modelled based on this data, are expressed as;

$$\tau_r = \frac{1}{9 \times \exp\left(\frac{V}{25.371}\right) + 1.3 \times \exp\left(-\frac{V}{13.026}\right)}, \quad (67)$$

$$\tau_s = \frac{1}{100 \times \exp\left(-\frac{V}{54.645}\right) + 656 \times \exp\left(\frac{V}{106.157}\right)}, \quad (68)$$

The I_{Kr} current trace could then be produced using the newly modified equation for this current;

$$I_{Kr} = 0.014 \times r \times s \times (V - E_K), \quad (69)$$

Putting all this together gives us the following relationships (Figure 17);

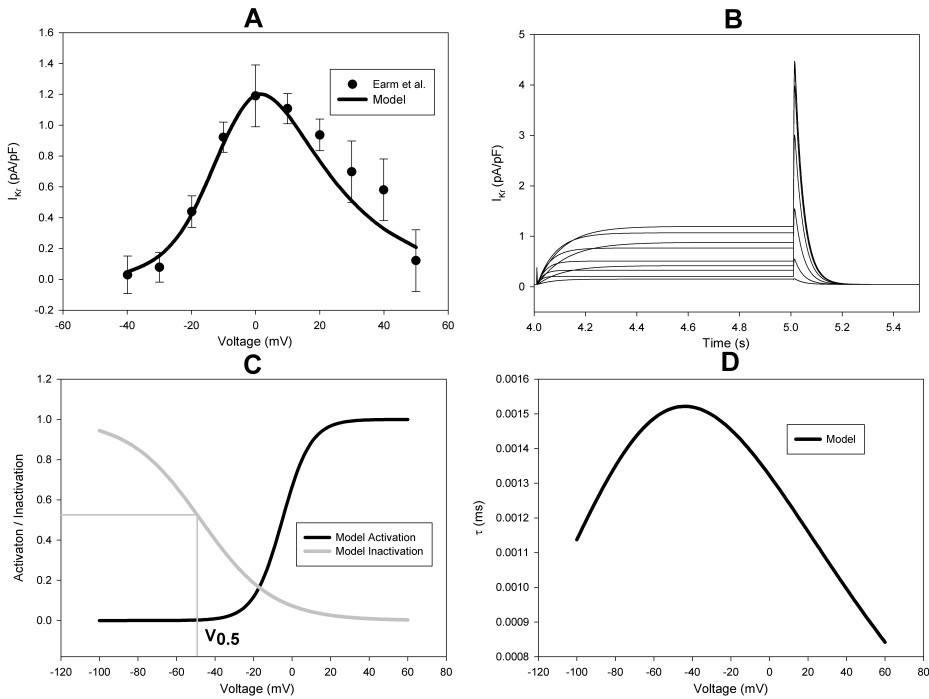


Figure 17: A)Current-Voltage curve for I_{K_r} in the pulmonary vein; B)Current traces for isolated cells from a holding potential of -90 mV with 10 mV depolarising steps to voltages from -50 to +50 mV; C)Activation-Inactivation curves and D)time constant

3.3.5. Inward rectifier potassium current, I_{K_1}

I_{K_1} kinetics are simple with no activation or inactivation variables. I_{K_1} was adjusted to fit experimental data from Chen (2006) and a current trace produced using the newly modified equation for this current;

$$I_{K_1} = \frac{3.271 \times (V - E_K - 12)}{\left(1 + \exp\left(\frac{1.393 \times F}{RT} \times (V - E_K - 12)\right)\right) + 0.05}, \quad (70)$$

This gives us the following relationships (Figure 18);

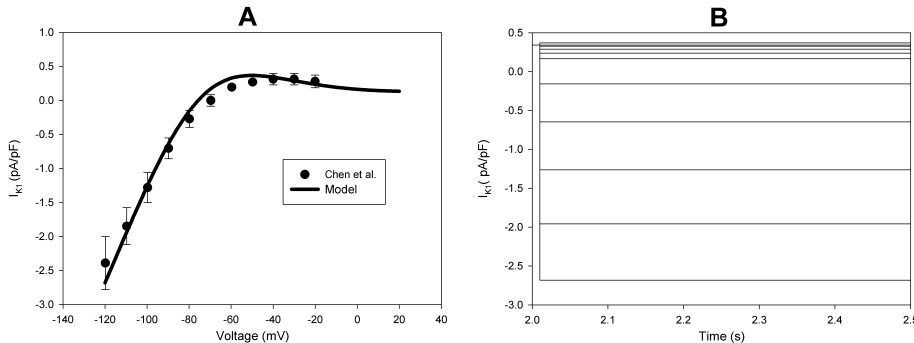


Figure 18: A)Current-Voltage curve for I_{K_1} in the pulmonary vein; B)Current traces for isolated cells from a holding potential of -40 mV with 10 mV depolarising steps to voltages from -120 to -20 mV

3.3.6. Action Potential

Individual currents for PV were combined in the whole cell model. The sustained outward current was included in our code and altered until our modelled AP agreed well with that found experimentally by Boyden (2007).

$$I_{out} = 0.5 \times (V + 85), \quad (71)$$

The final AP simulated at BCL=400ms is shown below (Figure 19).

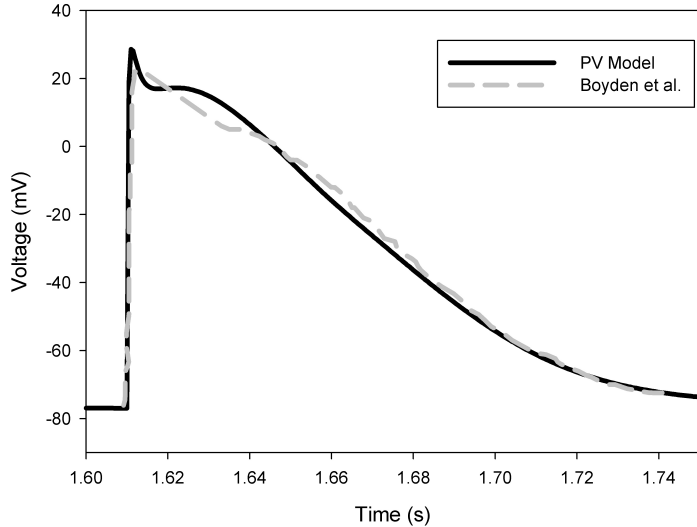


Figure 19: The simulated (black solid) and recorded (grey dash) action potentials for the pulmonary vein. Resting potential -76 mV, APD 109 ms APA 100 at BCL 400ms (c.f. Boyden et al. Resting potential -76 mV, APD 107 ms, APA 100 mV)

4. Discussion

The aim of this project was to develop a mathematical model of the rabbit cardiomyocytes that comprise the main interatrial conduction pathways and the pulmonary vein, based on single-cell voltage clamp data. Such models, providing detailed description of underlying ionic currents, are essential for understanding the electrophysiology of the heart as a whole. A rabbit model is particularly useful as rabbit hearts are structurally very similar to human hearts and rabbit data is easier to obtain from experiment for obvious reasons. (Lindblad 1996)

4.1. Restitution Curves

By comparing Figures 11, 14 and 20 we can see that the differences between AP's for these cell types have been modelled well. These differences can be investigated further by considering the restitution curves; a measure of the dependence of APD on BCL (Figure 20).

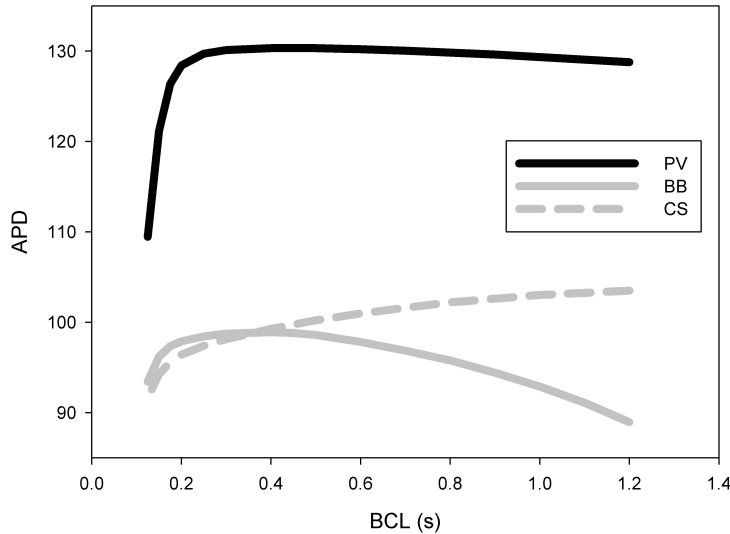


Figure 20:
Restitution curves
for the pulmonary
vein (black)
coronary sinus (gray
dashed) and
Bachmann's bundle
(gray solid)

The figure shows quite clearly that for all cell types the relation between BCL and APD holds for physically reasonable BCL. As BCL increases, the differences in the APD and therefore underlying physiology of BB and PV become more significant. We have produced a reliable group of models has been with the ability to reproduce results from experimental data despite there being very little data available for some currents. These models can be used to investigate simulate electrophysiological events within rabbit interatrial conduction pathways as well as the pulmonary vein. They could be used to investigate effects of different drugs on individual ion currents of combined with models for other cell types to create a model for the whole rabbit heart. Our model for the pulmonary vein is especially useful as it can now form the basis for an investigation into the electrophysiological basis of arrhythmias. The underlying causes of atrial fibrillation are of particular interest and Section B of this report details the beginnings of our work in this area.

B. SPONTANEOUS ACTIVITY IN THE PULMONARY VEIN

1. Introduction

Atrial fibrillation is a cardiac arrhythmia where electrical impulses generated by the sinoatrial node are overwhelmed by disorganized electrical impulses that originate in the atria and pulmonary veins, disturbing normal conduction pathways and adversely effecting contraction, particularly in the ventricles. Electrophysiology studies have suggested that high frequency activity in the pulmonary vein is an important factor in the initiation and perpetuation of atrial fibrillation but there is no consensus as to how this activity is initiated. (Chou 2008)

1.1. Receptor Gated Ion Channels and Calcium Dynamics

It has been shown in tissue samples that by inhibiting Ryanodine receptors, RyRe, in the sarcoplasmic reticulum, the pulmonary vein can be made to act as an ectopic pacemaker. The AP changes from that of a typical pulmonary vein cell to something resembling a cell from the sinoatrial node, with elevated plateau, depolarised RP and the beginnings of pacemaker depolarisation which became more marked after a period of rapid pacing. (Honjo 2003) This suggests that a major cause of spontaneous activity is alterations to intracellular calcium dynamics.

There are ion channels in the membrane of the SERCA just as there are in the cell membrane (*Figure 5*), gated in much the same way as described in Section A except that instead of responding to changes in voltage, these channels respond to chemical signals. (Katz 2001) When I_{CaL} is initiated during phase 2 of the AP calcium enters the cell from the extracellular medium. These calcium ions bind to specific sites on the membrane of the SERCA and open the transmembrane calcium channels causing a release of extra calcium into the cell via the release current I_{rel} . The calcium binding sites are the RyRe referred to above and by inhibiting them the release channel is effectively blocked reducing the amount of calcium that enters the cell and therefore the intracellular calcium concentration, $[Ca]_i$. (Honjo 2003) I_{CaL} deactivates rapidly but if $[Ca]_i$ is low it may reactivate before the AP fully repolarises, causing early afterdepolarisation, EAD shown in *Figure 22 left*. (Bers 2002)

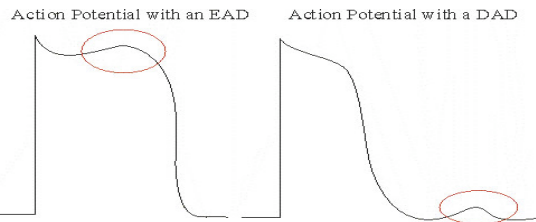


Figure 21: Right, atrial action potential showing evidence of EAD. Left, atrial action potential showing DAD.

(Imperial 2008)

1.2. Calcium Activated Currents

Blocking RyRe causes an increase in calcium concentration within the SERCA, which eventually becomes over-filled initiating spontaneous calcium release. This sudden increase in intracellular calcium is countered by a calcium activated transient depolarising inward current, I_{ti} , 90% of which is attributed to I_{NaCa} discussed briefly in Section A, with the other 10% attributable to a calcium activated chloride current, I_{ClCa} . The depolarising action of these currents is seen as a small bump after the AP. (*Figure 21 right.*) This bump resembles pacemaker depolarisation, which could bring the membrane potential to the threshold of I_{Na} , triggering a new AP. (Schlotthauer 2000)

1.3. Initiation of Normal Pacemaker Activity

When considering spontaneous activity it is sensible to consider its causes in normal pacemaker activity in the sinoatrial node. Here the most important currents are I_{CaT} and the hyperpolarising activated current, I_f , which is fully active at around 80mV, near the RP. It is thought that these currents are responsible for initial pacemaker depolarisation during phase 4, which brings the membrane potential to the threshold of I_{Na} whereupon it activates and begins phase 0. One study using pulmonary vein cells that demonstrated spontaneous activity, including pacemaker depolarisation in phase 4, failed to find any evidence of I_{CaT} . They did find a hyperpolarising activated current but its reversal potential was far more negative than expected and they suggest that it is not I_f but rather I_{KH} , a hyperpolarising and time-dependent current previously reported in canine pulmonary vein cells. (Earm 2008)

2. Computer Modelling Methods

The main goal of this section was to develop our model of the pulmonary vein into one that could accurately simulate the electrophysiology of PV cells that exhibit spontaneous activity and thereby identify its main cause. As with Section A we took data from physiological experiments involving spontaneous activity in PV and used this to construct new currents based on the theories introduced above.

Calcium dynamics in this model are taken from Lindblad et al. This simulates the SERCA in the form of two chambers with a release current, I_{rel} , uptake current, I_{up} and the transfer current I_{tr} . I_{rel} moves calcium out of the

store from the release compartment, I_{up} takes calcium into the uptake compartment and I_{tr} moves calcium between the two. (Lindblad 1996)

3. Results

3.1. Hyperpolarising Activated Current, I_f

I_f is modelled based on data from Earm (2008) with one activation variable (r), and a corresponding time constant (τ). The activation is expressed as;

$$r = \frac{1}{1 + \exp\left(\frac{(V + 85.6)}{6.8}\right)}, \quad (72)$$

The activation time constant is;

$$\tau = \frac{4}{(\exp(-2.9 - (0.04 \times V)) + (\exp(3.6 + (0.11 \times V))))}, \quad (73)$$

The complete expression for I_f is;

$$I_f = 7.2827 \times \frac{dy}{dt} \times (V - E_{Na}), \quad (74)$$

$$\text{where } \frac{dy}{dt} = \frac{(y - r)}{\tau}. \quad (75)$$

I_f was not found to initiate spontaneous activity but did appear to effect the form of the action potential during diastole, specifically the appearance of pacemaker depolarisation, but only for very large values of I_f .

3.2. Calcium Activated Currents

It has been suggested that as much as 30% of I_{ti} may be attributed to the calcium-activated chloride current I_{ClCa} , (Zygmunt 1998) though more recent papers have suggested 10% at most. This can be seen because blocking the chloride channel abolishes pacemaker activity. (Honjo 2003) Chloride does not undergo independent activation or inactivation and so we model it as a purely calcium-dependent current as in Earm (2006). The current is expressed as;

$$I_{ClCa} = 435.93 \times \frac{VF}{RT} \times \frac{\left(([Ca]_i - 2) \times \exp\left(\frac{VF}{RT}\right) \right)}{\left(1 - \exp\left(\frac{VF}{RT}\right) \right)} \times y_i^{1.7}, \quad (76)$$

$$\text{where } y_i = \frac{K_f \times [Ca]_i^{1.7}}{K_f \times [Ca]_i^{1.7} + K_b \times \left(\frac{K_b}{K_f}\right)^{1.7}}. \quad (77)$$

$K_b = 100$ and $K_f = 665.78$, are constants. I_{ClCa} does not adversely affect the AP, in fact it does not appear to have any effect at all. We suggest that this is because I_{ClCa} is a small current that is only observed at unphysically high extracellular sodium concentrations.

With I_{ClCa} shown to be of little importance we consider I_{NaCa} , which was modelled based on data taken from PV cells that had already been shown to be self oscillating. I_{NaCa} does not undergo independent activation or inactivation and so we model it as a purely calcium-dependent current as in Chen (2006). The current is expressed as;

$$I_{NaCa} = \left(\frac{0.02 \times [Na]_i^3 \times 7.5 \times \exp\left(0.35 \times \frac{VF}{RT}\right) - 140^3 \times [Ca]_i \times \exp\left((0.45 - l) \times \frac{VF}{RT}\right)}{1.0003 \times ([Ca]_i \times 140^3 + 2.5 \times [Na]_i^3)} \right) - 0.5, \quad (78)$$

The inward component of I_{NaCa} that arises from the form expressed in equation (78) is increased compared to that found in normal PV cells. This appears to be the primary factor in spontaneous activity. (Hancox 2008)

3.3. Sustained Spontaneous Activity

The grey trace on the left in *Figure 22* shows a series of spontaneous action potentials generated after a single stimulus. It does not agree with that found in experiments, the period of oscillation is around 1s, the APA is 20mV and the RP is -70mV (c.f. Earm 2008). There is also no sign of pacemaker depolarisation. By altering the calsequestrin buffer, which in turn changes calcium dynamics (*Figure 22 right*) we were able to produce the black trace in on the left in *Figure 22*. It shows all the expected features of spontaneous activity including pacemaker depolarisation.

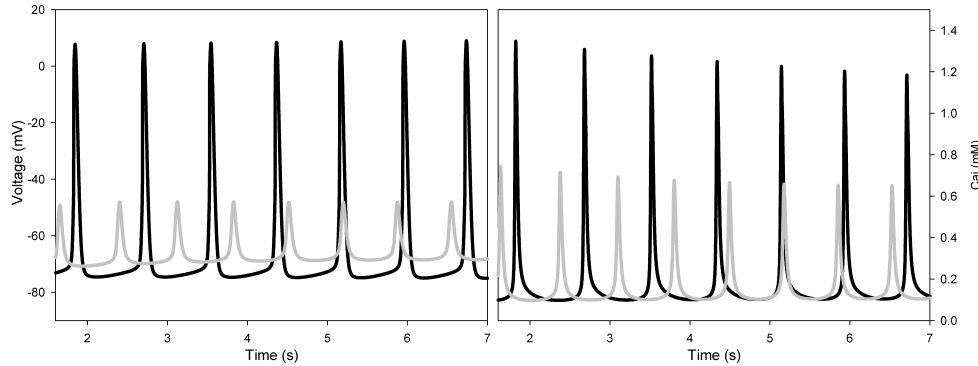


Figure 22:
Spontaneous activity in PV cells (left panel), with (black) and without (grey) altered calsequestrin, and their respective Ca^{2+} transients.

4. DISCUSSION

It seems that spontaneous activity is largely dependent on calcium activated currents, in particular I_{NaCA} , with I_f playing only a minor role. Attempts were made to rectify the APA, APD and RP using the fluxes available to us in the Lindblad model, I_{rel} , I_{tr} and I_{up} , but these were unsuccessful. This is a problem inherent in the Lindblad model of calcium dynamics which may be solvable by using the model of calcium dynamics suggested by Shannon (2004), a more robust model which accounts for more physically observable attributes than Lindblad.

There is evidence to suggest that the calcium transient seen during AP is caused by the AP as opposed to the transient causing the AP (Hancox 1994). It is interesting to note that in our model the opposite seems to be true, as we have a situation where the calcium transient exists in the absence of any AP (*Figure 23*). This may be a result of limitations in the Lindblad model and merits further investigation using the Shannon model.

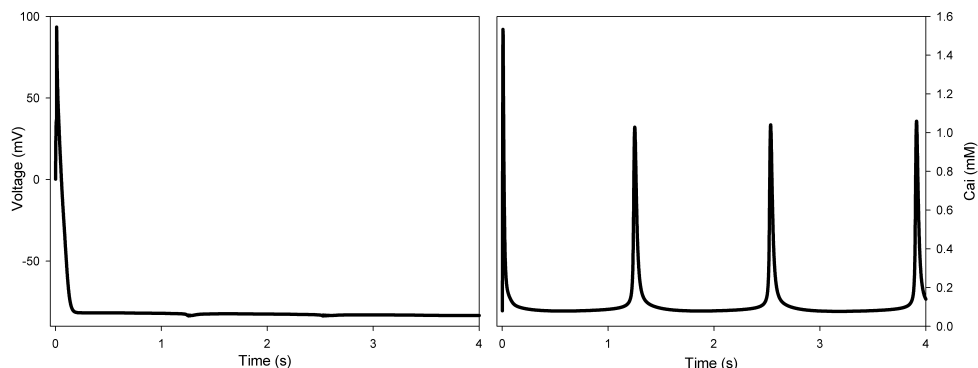


Figure 23:
Spontaneous Ca^{2+} transients (right) generated in the absence of AP activity (left)

ACKNOWLEDGEMENTS

We would like to thank members of the Biological Physics Group at the School of Physics and Astronomy for all their help and encouragement throughout this project and for giving us the opportunity to return next semester. Special thanks to Dr Oleg Aslanidi for putting up with us.

REFERENCES

- Berne, A., Levy, M. (1999). *Principles of Physiology* 3rd Edition. Philadelphia: Elsevier.
- Bers, D. (2002). Calcium and Cardiac Rhythms: Physiological and Pathophysiological. *Circulation Research* **90**, 14-17.
- Boyden, P. A., Dun, W., Ozgen, N., Hirose, M., Sosunov, E. A., Anyukhovsky, E. P., Rosen, M. R. (2007). Ionic Mechanisms Underlying Region-Specific Remodeling of Rabbit Atrial Action Potentials Caused by Intermittent Burst Stimulation. *Heart Rhythm*, **4** (4), 499-507.
- Chen, Y., Chen, S., Chen, Y., Tai, C., Chan, P., Lin, C. (2004). T-type Calcium current in Electrical Activity of Cardiomyocytes Isolated from Rabbit Pulmonary Vein. *J Cardiovasc Electrophysiol*, **15** (5), 567-571.
- Chen, Y., Chen, Y., Chang, C., Wongcharoen, W., Yeh, H., Chen, S. (2006). Effects of a Na^+/Ca Exchanger Inhibitor on Pulmonary Vein Electrical Activity ans Ouabain-induced Arrhythmogenicity. *Cardiovascular Research* **70**, 497-508.
- Chen, Y., Lee, H., Chen, Y., Chang, S., Tai, C., Wongcharoen, W., Yeh, H., Lin, C., Chen, S. (2007). Tumor Necrosis factor- α alters calcium handling and increases arrhythmogenesis of pulmonary vein cardiomyocytes. *Life Sciences* **80**, 1806-1815.

- Chou, C., Chen, P., Lin, S. (2008). Intracellular Calcium Dynamics and Atrial Fibrillation. A. Natale, J. Jalife (eds.) *Contemporary Cardiology: Atrial Fibrillation. From Bench to Bedside*. Totowa: Humana Press.
- Earm, Y., Seol, C., Kim, J., Kim, W., Ha, J., Choe, H., Jang, Y., Shim, E., Youm, J., Leem, C. (2008). Simulation of Spontaneous Action Potentials of Cardiomyocytes in Pulmonary Veins of Rabbits *Progress in Biophysics and Molecular Biology* **96**, 132-151.
- Guevara, M.R. (1991). Mathematical Modeling of the Electrical Activity of Cardiac Cells. L. Glass, P. Hunter, A. McCulloch (eds.) *Theory of Heart: Biomechanics, Biophysics, and Nonlinear Dynamics of Cardiac Function*. New York: Springer-Verlag.
- Hancox, J., Levi, A., Brooksby, P. (1994). Intracellular Calcium Transients Recorded with Fura-2 *Proc Biol Sci* **255**, 99-105.
- Hancox, J., Ridley, J., Cheng, H., Harrison, O., Jones, S., Smaith, G., Orchard, D. (2008). Spontaneous Frequency of Rabbit Atrioventricular Nonde Myocytes Depends on SR Function *Cell Calcium* **44**, 580-591.
- Honjo, H., Boyett, M., Niwa, R., Inada, S., Yamamoto, M., Mitsui, K., Horiuchi, T., Shibata, N., Kamiya, K., Kodama, I. (2003). Pacing Induced Spontaneous Activity in Myocardial Sleeves of Pulmonary Veins After Treatment With Ryanodine. *Circulation*, **107**, 1937-1943.
- Imperial College London (2008). Glossary of Terms [Website]. Available from: <<http://www1.imperial.ac.uk/medicine/about/divisions/nhli/cardio/heart/molcell/ccir/glossary/>> [Accessed: 13 January 2009].
- Katz, A. M. (2001). *Physiology of the Heart*. 3rd Edition. Philadelphia: Lippincott, Williams & Wilkins.
- Klaubund, R. E. (2005). *Cardiovascular Physiology Concepts*. Philadelphia: Lippincott, Williams & Wilkins.
- Lindblad, D. S., Murphey, C. R., Clark, J. W., Giles, W. R. (1996). A Model if the Action Potential and Underlying Membrane Currents in a Rabbit Atrial Cell *Am J Physiol* **271**, H1666-1696.
- Lloyd, C. (2001) Clancy-Rudy Markovian Model of Ion Channels [Website]. Available from: <http://www.cellml.org/examples/repository/CR_model_2001_doc.html> [Accessed: 14 January 2009].
- Medscape (2003). Drug Related QT Interval Prolongation. *Pharmacotherapy* **23**(7), 881-908.
- Sakamoto, S., Nitta, T., Ishii, Y., Miyagi, Y., Ohmori, H., Shimizu, K. (2005). Interatrial Electrical Connections: The Precise Location and Preferential Conduction. *J Cardiovasc Electrophysiol*, **16**, 1077-1086.
- Schlotthauer, K. (2000) Sarcoplasmic Reticulum Ca²⁺ Release Causes Myocyte Depolarisation: Underlying Mechanism and Threshold for Triggered Action Potentials *Circulation Research* **87**, 774-780.
- Shannon, T., Wang, F., Puglisi, J., Weber, C., Bers, D. (2004) A Mathematical Treatment of Integrated Ca Dynamics within the Ventricular Myocyte *Biophysical Journal* **87** (5), 3351-3371.
- Zygmunt, A., Gibbons, W. (1992) Properties of the Calcium-activated Chloride Current in Heart *J Gen Physiol* **99**, 391-414.
- Zygmunt, A., Goodrow, R., Weigel, C. (1998). INaCa and ICICa Contribute to Isoproterenol-induced Delayed Afterdepolarisations in Midmyocardial Cells *Am J Physiol Heart Circ Physiol* **275**, H1979-1992.